SUPPLEMENTARY INFORMATION

Hybrid Core-Shell Nanoparticles for Cell-Specific Magnetic Separation and Photothermal Heating

Cristina de la Encarnación[#a,b], Felix Jungwirth[#a,c], David Vila-Liarte[a,d], Carlos Renero-Lecuna[a,d], Safiyye Kavak[e], Iñaki Orue[f], Claire Wilhelm[g], Sara Bals[e], Malou Henriksen-Lacey[a,d], Dorleta Jimenez de Aberasturi*[a,d,h], Luis M. Liz-Marzán*[a,d,h]

[#]*These authors contributed equally*

[a] CIC biomaGUNE, Basque Research and Technology Alliance (BRTA), 20014 Donostia-San Sebastián, Spain

[b] Department of Applied Chemistry, University of the Basque Country, 20018 Donostia-San Sebastián, Spain

[c] Goethe-Universität Frankfurt, Physikalisches Institut, 60438 Frankfurt am Main, Germany

[d] Centro de Investigación Biomédica en Red de Bioingeniería, Biomateriales y Nanomedicina (CIBER-BBN), 20014 Donostia-San Sebastián, Spain

[e] EMAT and NANOlab Center of Excellence, University of Antwerp, Antwerp, Belgium

[f] SGIKER, Servicios Generales de Investigación, University of the Basque Country, 48940 Leioa, Spain

[g] Laboratoire Physico Chimie Curie, PCC, CNRS UMR168, Institut Curie, Sorbonne University, PSL University, Paris, 75005 France

[h] Ikerbasque, Basque Foundation for Science, 48009 Bilbao, Spain

*e-mail: djimenezdeaberasturi@cicbiomagune.es (D.J.A.); llizmarzan@cicbiomagune.es (L.M.L.-M.)

Contents

1. Synthesis of silica@iron oxide nanoparticles

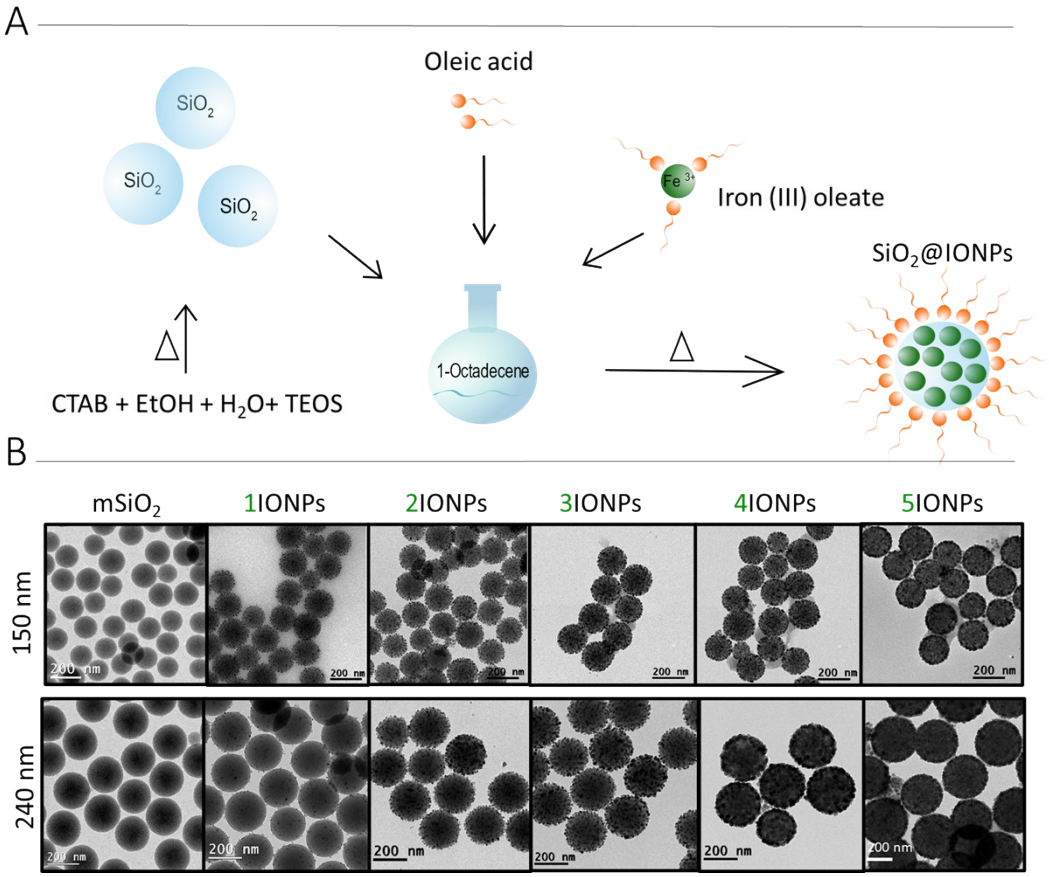

Figure S1. **(A)** Schematic representation of the synthesis used to obtain IONP-decorated mesoporous silica core-shell particles. **(B)** TEM images of SiO_2@IONPs at different overgrowth steps, for two different silica sizes (150 and 240 nm, as labelled). The numbers in green indicate the number of thermal decomposition steps for each sample.

2. Characterisation of silica@iron oxide nanoparticles

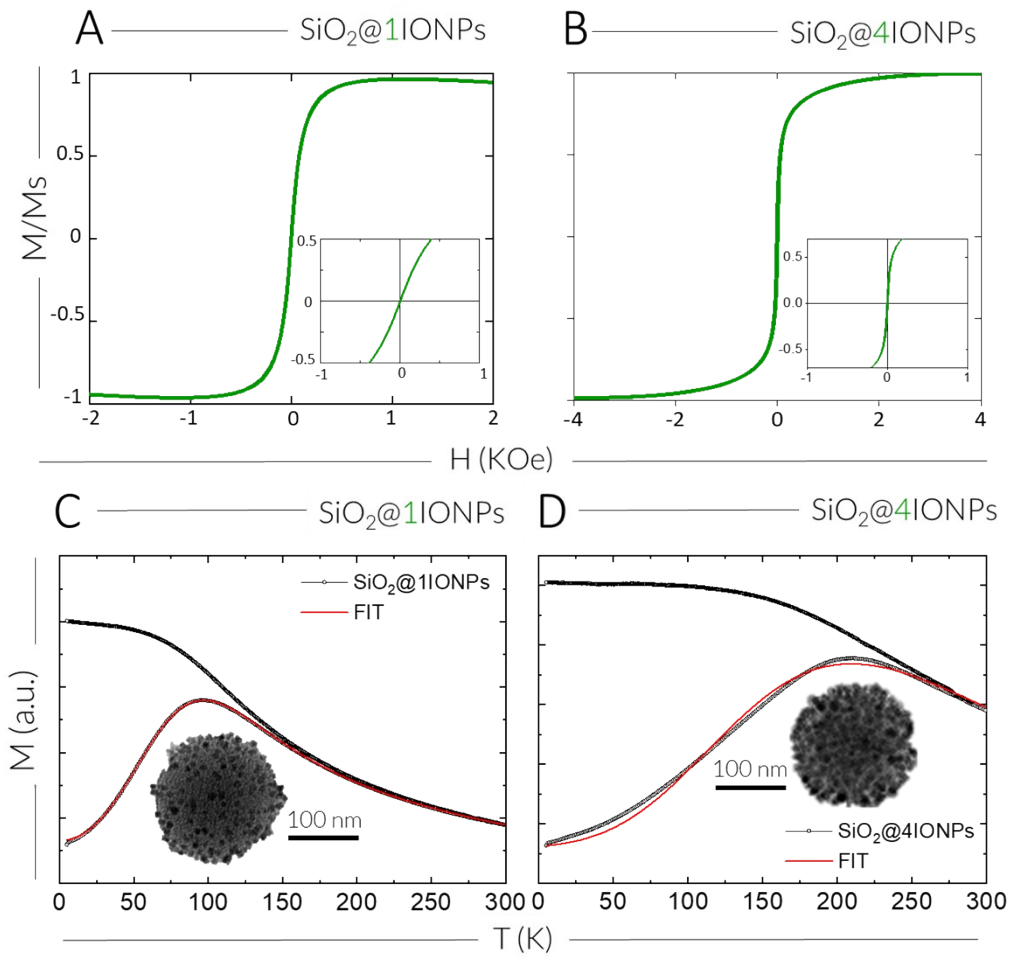

Figure S2. (A,B) Hysteresis loops for SiO_2@1IONPs **(A)** and SiO_2@4IONPs **(B)**. **(C,D)** ZFC/FC curves for SiO_2@1IONPs **(C)** and SiO_2@4IONPs **(D)**. TEM images are included showing the difference in the size and density of the IONPs.

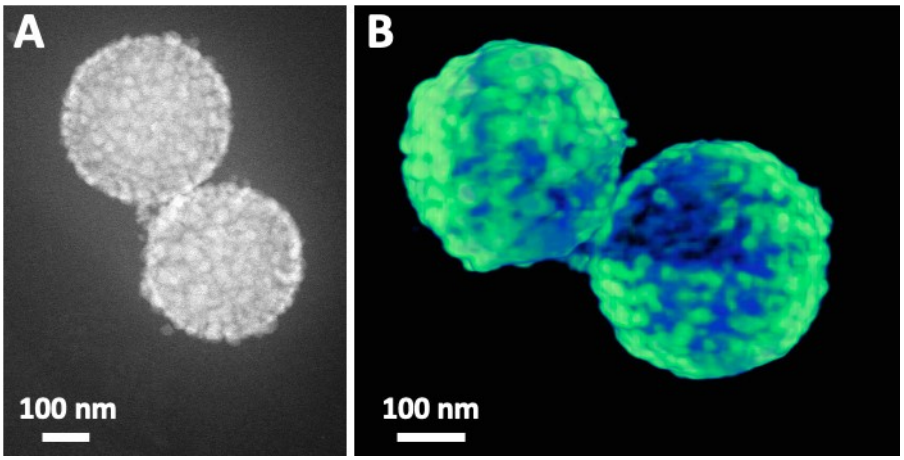

Figure S3. (A) Representative ADF-STEM image of SiO_2@IONPs. (B) Snapshot from a 3D electron tomography reconstruction of SiO_2@IONPs.

3. Characterisation of gold nanorods@silica@iron oxide nanoparticles

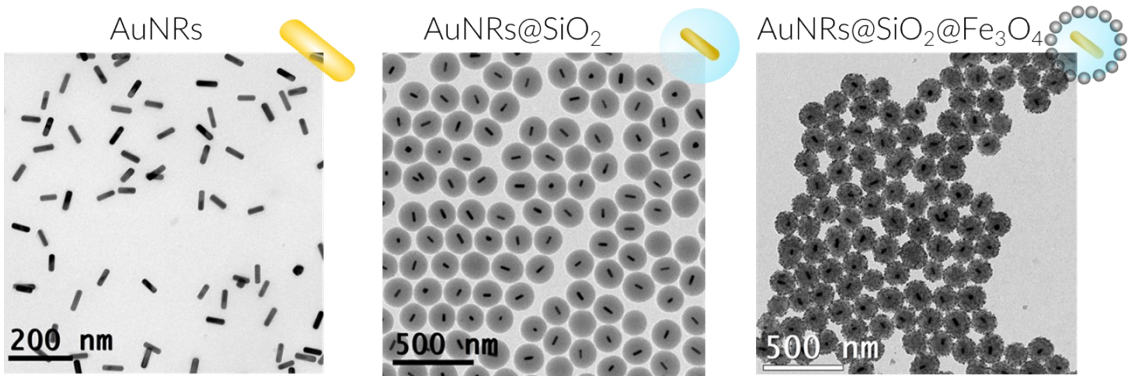

Figure S4. Low magnification TEM images of AuNRs, AuNR@SiO_2 and AuNR@SiO_2@IONPs.

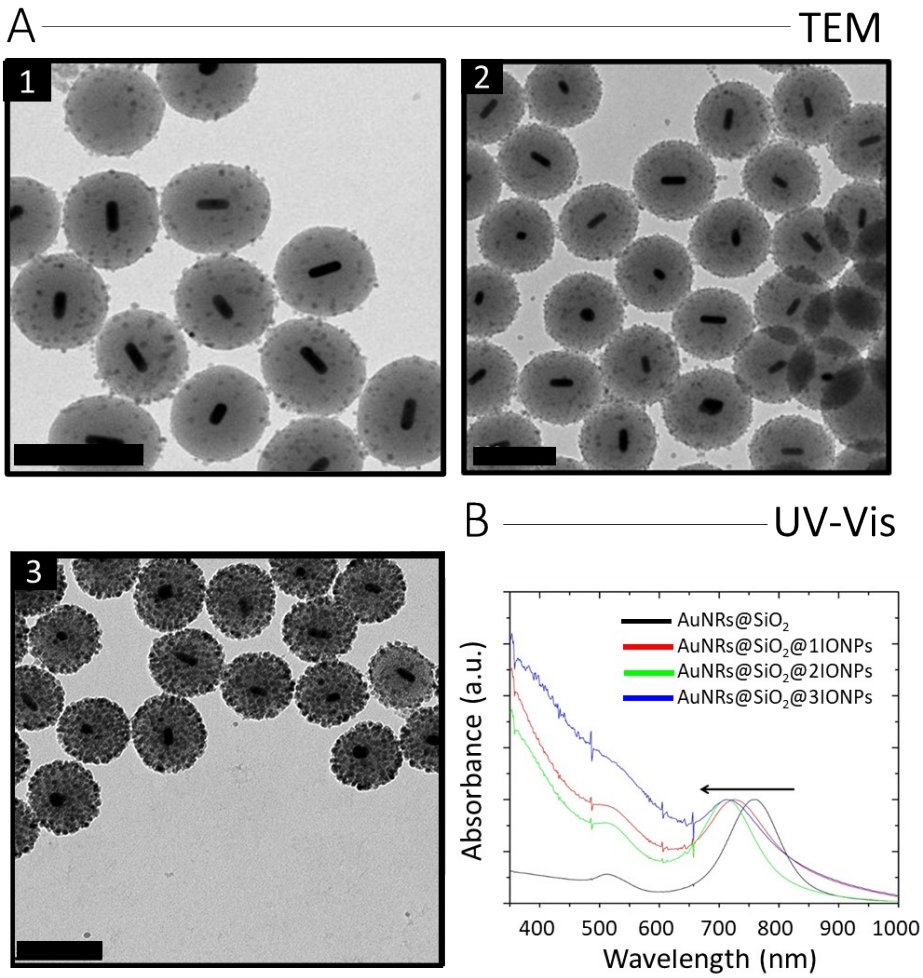

Figure S5. (A) TEM images of the IONP covered AuNR core mesoporous silica shell particles after different steps of overgrowth. AuNR@SiO_2 after **(1)** first decomposition step (10 min holding time), some small IONPs are attached to the mesoporous silica **(2)** second decomposition step (30 min) **(3)** third decomposition step (30 min). Scale bar 200 nm. **(B)** UV-VIS spectra of AuNRs@SiO_2@Fe_3O_4 at different Fe_3O_4 overgrowth steps. Reshaping of the AuNRs, indicated by a blue shift of the LSPR band from 760 nm to 730 nm can be observed for increasing number of decomposition steps. All the spectra were normalized at the LSPR peak maximum.

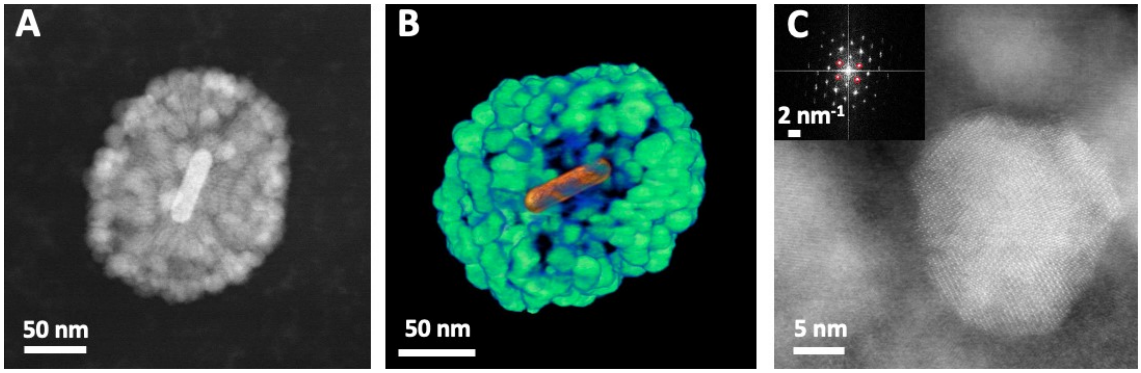

Figure S6. (A) Representative ADF-STEM image of AuNR@SiO_2@Fe_3O_4. (B) Snapshot from a 3D electron tomography reconstruction of AuNR@SiO_2@Fe_3O_4, in which inpainted ADF-STEM, and HAADF-STEM data are used together. (C) HRSTEM image of IONPs on the silica surface, and fast Fourier transform (FFT) (inset) where red circles represent the reflections from {111} families attributed to Fe_3O_4.

4. Magnetic separation

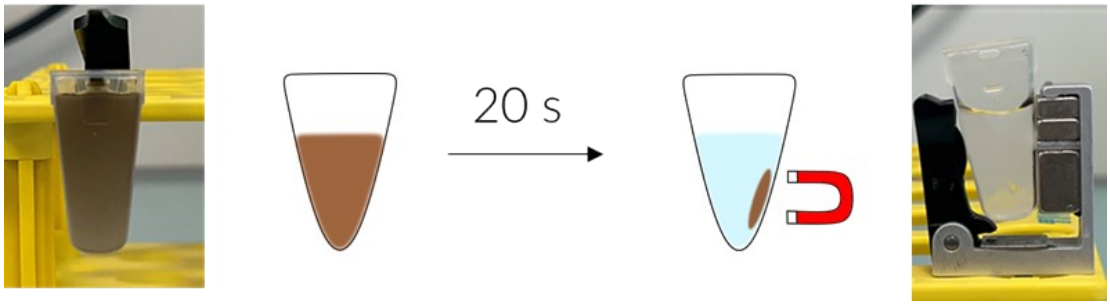

Figure S7. Schematic representation and real pictures showing magnetic separation. The AuNRs@SiO_2@IONPs aqueous dispersion was placed in a plastic vial (left) and a permanent magnet was placed on the side of the vial. The AuNRs@SiO_2@IONPs were magnetically separated and concentrated into a brown pellet (right).

5. Optical density

Table S1. Optical density at 808 nm of AuNRs@SiO_2 (red), SiO_2@4IONPs (green) and AuNRs@SiO_2@IONPs (blue) measured using a UV-Vis-NIR spectrometer.

Optical density

[Au] mM	OD_{808}
0.005	0.007
0.01	0.009
0.02	0.03
0.05	0.1
0.1	0.34

[Fe] mM	OD_{808}
0.3	0.04
0.5	0.06
1.0	0.09
2.6	0.27
5.2	1.12

[Au] mM	[Fe] mM	OD_{808}
0.005	0.3	0.15
0.01	0.5	0.24
0.02	1.0	0.42
0.05	2.6	0.77
0.1	5.2	1.46

6. Characterisation of AuNR@SiO_2@IONP association with cells

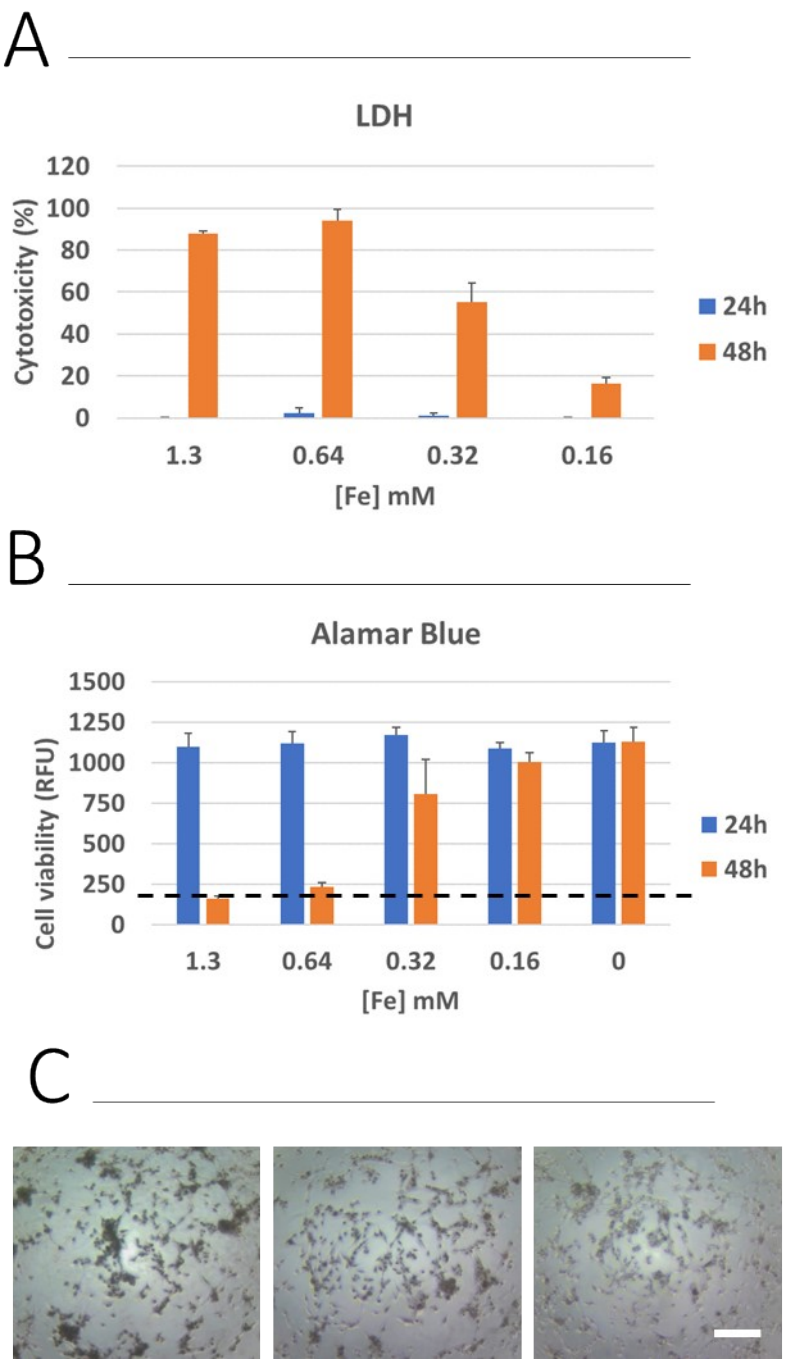

Figure S8: Cell viability of U87 cells after exposure to AuNRs@SiO_2@IONP NPs for 24h or 48h (right). Results from both the LDH (A) and Alamar Blue (B) cell viability assays are shown. Mean ± SD of triplicate measurements. The black dotted line indicates 100% cell death in the Alamar blue assay. (C) Brightfield images showing U87 cells after 24h incubation with AuNRs@SiO_2@IONP NPs at 1.3, 0.64 and 0.32 mM [Fe]. Scale bar: 500 µm.

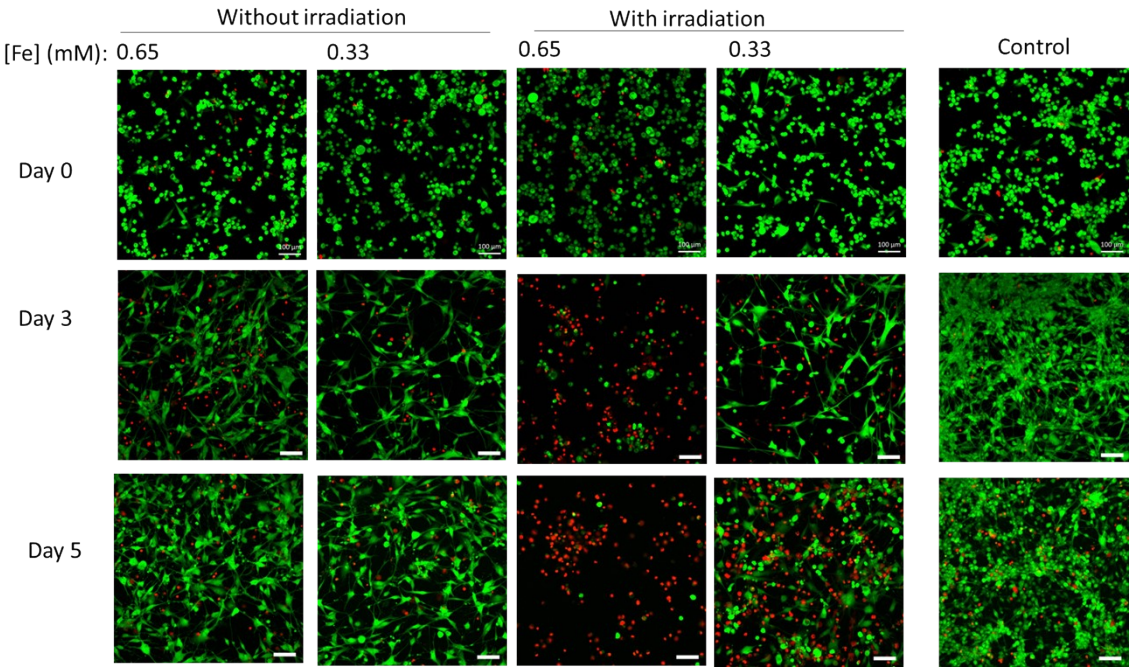

Figure S9: Live/dead fluorescent staining of U87 cells exposed to AuNR@SiO_2@IONPs (0.33 and 0.65 mM [Fe], equivalent to 6.3 and 12.5 µM [Au], respectively) for 24h, followed by removal of non-endocytosed NPs and laser irradiation. Timepoints represent days post irradiation. A multi-mode laser with 4 mm spot size was used, applying 12 W/cm^2 for 5 min. Live cells stain green and dead cells stain red. Furthermore, the native morphology of U87 cells can be used as an indicator of cell health. All scale bars: 100 µm.

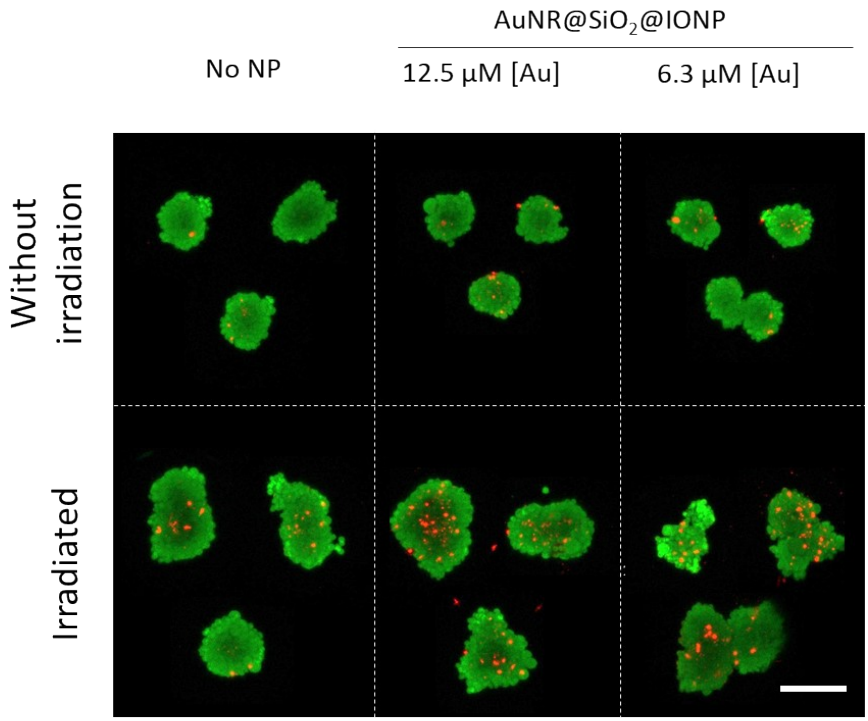

Figure S10. Composite images of spheroids, with and without irradiation, after being exposed to AuNR@SiO_2@IONPs for 24h. A multimode laser with 4 mm spot size was used, applying 16 W/cm^2 for 5 min. Live/Dead cell staining was conducted 24 h post irradiation. Scale bar: 200 µm.

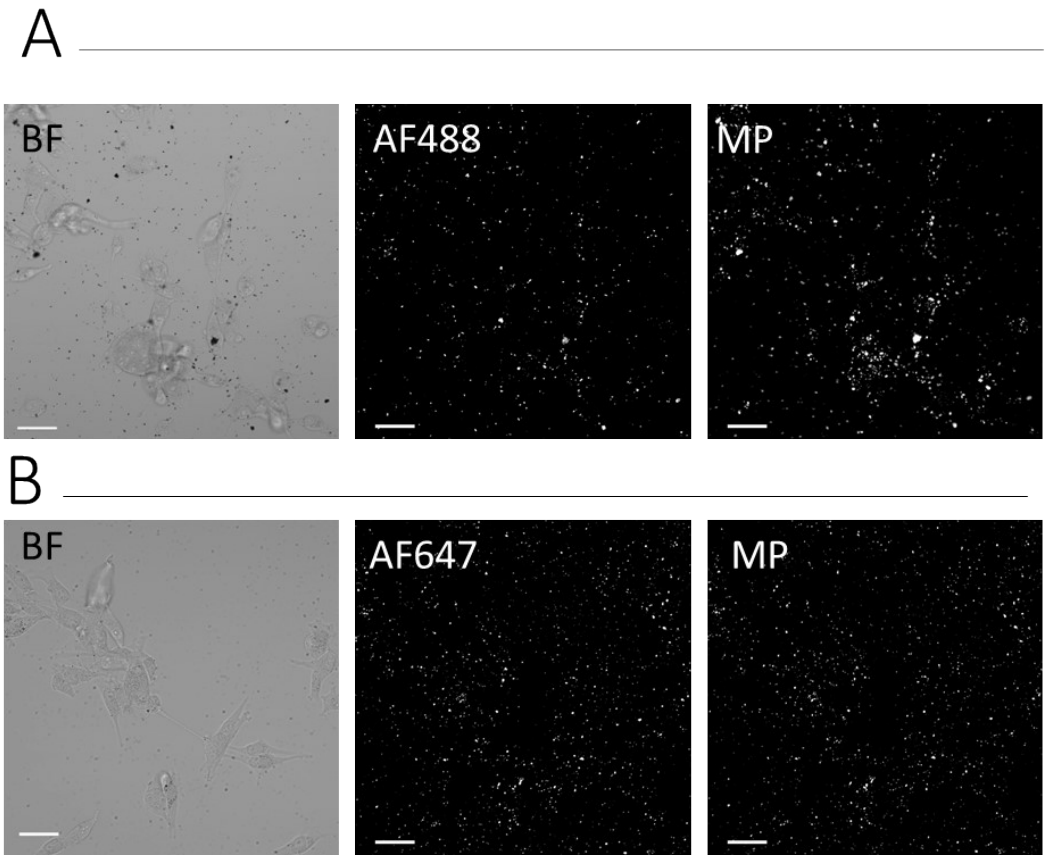

Figure S11: Direct and Indirect immunofluorescence of CD44 targeted AuNR@SiO_2@IONP-AB NPs. (A) Direct staining approach in which AF488 labelled CD44 is attached to NPs; (B) Indirect staining approach in which non-labelled CD44 is attached to NPs and post fixation AF647 anti-rabbit secondary antibody added. Both fluorescence and MP images are maximum intensity projections of ca. 25 µm thick z-stacks. Scale bars: 50 µm.

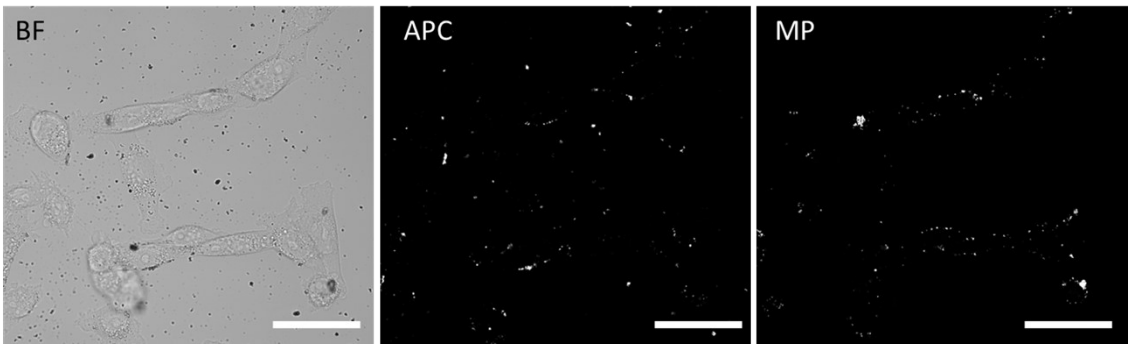

Figure S12: Detection of CD44-expressing MDA-MB.231 cells via AuNR@SiO_2@IONP-AB-APC exposure for 2h. In this case, an APC-labelled Rat CD44 antibody was used (BD Pharmingen 559250). Brightfield (BF), APC fluorescence (633nm ex), and multiphoton (MP) imaging are all shown. Scale bars: 50 µm.

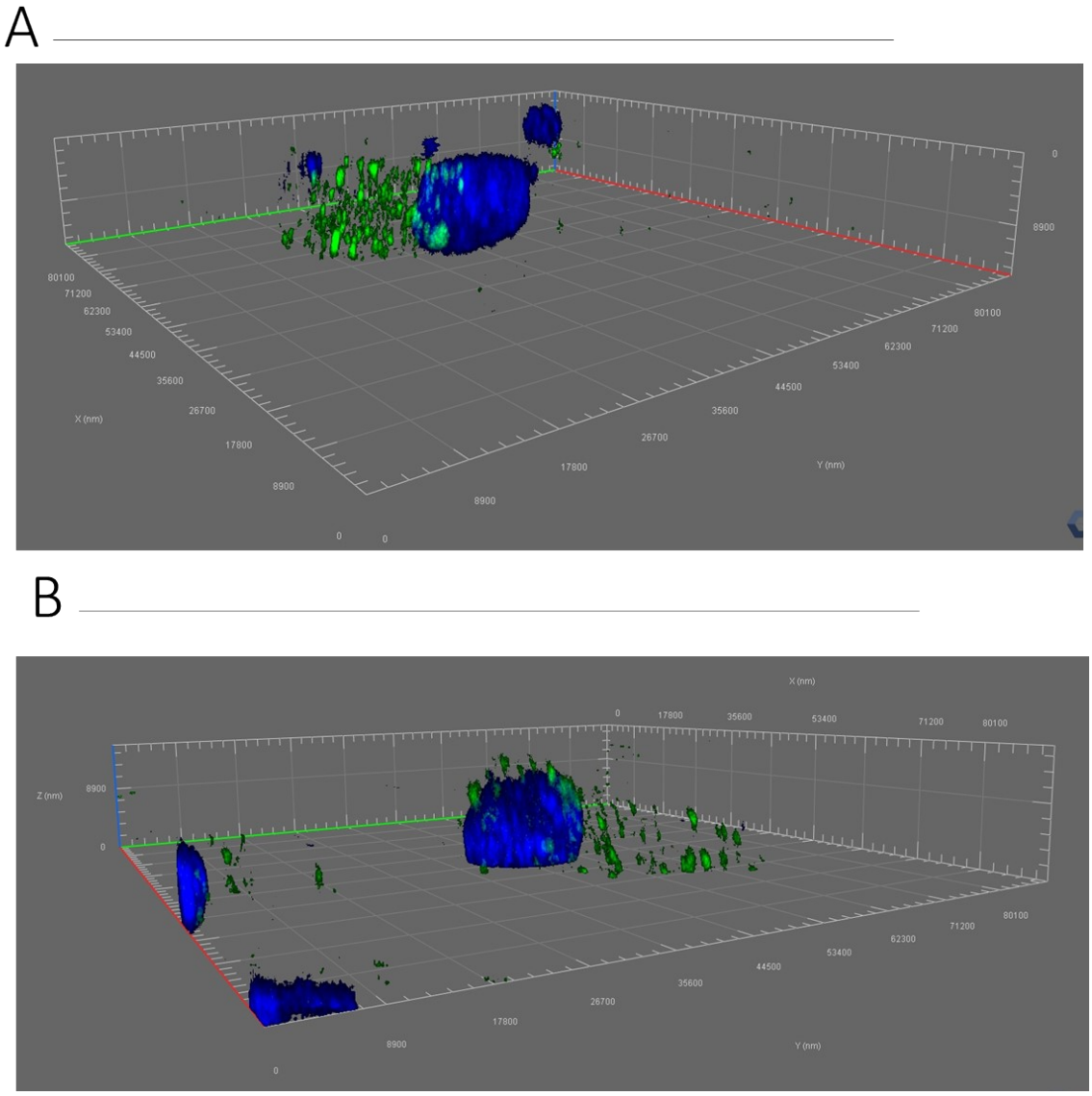

Figure S13. 3D reconstructions of a single U87 cell expose to AuNR@SiO_2@IONPs for 24h (A) or AuNR@SiO_2@IONP-AB for 2h (B). Differences in the cellular location can be observed, showing high levels of intracellular NP clustering in the case of non-antibody labelled NPs (A), and a more surface expression in the case of Ab-labelled NPs (B). NPs were imaged using MP confocal imaging and are falsely coloured in green, whereas the nucleus is shown in blue. A x40 oil objective (EC-Plan Neofluor) was used with ca. 265 nm pinhole to achieve a ca. 15 µm thick z-stack.